Domain Wall Creep in Magnetic Wires

F. Cayssol,[1] D. Ravelosona,[1,*] C. Chappert,[1] J. Ferré,[2] and J. P. Jamet[2]

[1]*Institut d'Electronique Fondamentale, UMR CNRS 8622, Université Paris Sud, 91405 Orsay Cedex, France*
[2]*Laboratoire de Physique des Solides, UMR CNRS 8502, Université Paris Sud, 91405 Orsay Cedex, France*

(Received 8 July 2003; published 10 March 2004)

The dynamics of a 1D domain wall (DW) in magnetic wires patterned in 2D ultrathin Co films is studied as a function of the wire width w_0. The DW velocity $v(H)$ is hugely reduced when w_0 is decreased, and its field dependence is consistent with a creep process with a critical exponent $\mu = 1/4$. The effective critical field scales as $(1/w_0)$. Measurements of $v(H)$ in wires with controlled artificial defects show that this arises from the edge roughness introduced by patterning. We show that the creep law can be renormalized by introducing a topologically induced critical field proportional to $(1/w_0)$.

DOI: 10.1103/PhysRevLett.92.107202 PACS numbers: 75.60.Ch, 68.35.Rh, 75.75.+a

Precise control of magnetization reversal in patterned magnetic nanostructures is a key parameter for future applications. Recently, it has been demonstrated [1,2] that magnetic elements could perform basic logic operations analogous to semiconductor electronics. The interest in magnetic logic devices lies in the growing importance of innovative schemes such as reprogrammable logic and reconfigurable computing [3]. A very promising scheme based on magnetic domain wall (DW) propagation in magnetic nanostructures has been proposed [1]. This new feature involves a precise driving of a DW in a nanoscopic circuit. Understanding how a DW propagates in small elements [4–6] is then of crucial importance.

In continuous magnetic films, the propagation process of a DW driven by a magnetic field results from the competition between an elastic energy that acts to straighten the DW and a quenched structural disorder which tends to roughen it by local pinning. Such a motion of an elastic object in the presence of weak disorder is involved in a wide range of systems [7–14]. In particular, the response of the system to a small external force f (well below the critical depinning force f_c) in the presence of thermal fluctuations is a very challenging problem. In that case, a weak pinning potential can lead to diverging barriers when $f \to 0$ [7,15] and a so-called nonlinear collective creep regime where the velocity is of the form $v \propto \exp[-\beta U_c (f_c/f)^{\mu}]$, where $\beta = 1/kT$ and U_c is a scaling energy constant. The exponent μ is characteristic of the disorder and of the dimensionality of the system. The creep law has been recently verified in 2D ultrathin magnetic films either in the presence of a quenched disorder [9] or in the presence of a correlated defect [10,11]. However, quantitative studies of creep phenomena in magnetic nanostructures are clearly needed since the reduction of lateral dimensions and additional pinning potential introduced by the patterning processes can lead to a very different behavior [16,17]. In that way, a 1D DW propagating in a patterned 2D ultrathin magnetic film is a very good model system to study the creep process in a confined 2D geometry.

In this Letter, we investigate the dynamics of a 1D DW in magnetic wires with a different width w_0 patterned in ultrathin magnetic films. For all widths, the DW motion is compatible with a creep process with a critical exponent $\mu = 1/4$. The effective critical field varies as $(1/w_0)$. We demonstrate that this arises from the edge roughness introduced by patterning. Our system is based on epitaxial Pt(3.4 nm)/Co(t_{Co})/Pt(4.5 nm)/Al_2O_3 ultrathin films showing high perpendicular anisotropy ($K_u \sim 1 \times 10^7$ ergs/cm^3) [18]. We focused our study on Co thicknesses $t_{\mathrm{Co}} = 0.5$ and 1 nm where dipolar effects are negligible. Since the thickness of the Co layer is much smaller than the DW width (~ 10 nm), DWs can be treated as Bloch walls where the effective anisotropy includes dipolar energy as $K_{\mathrm{eff}} = K_u - 2\pi M_S^2$ and M_S is the saturation magnetization [5,19]. These films can be considered as realistic 2D Ising systems because of narrow DWs, perpendicular orientation, and uniform magnetization across the film thickness. The pinning potential results mainly from very homogeneously distributed defects such as boundaries between crystallites and atomic steps at interfaces [18,20]. These defects can be considered as weakly pinning point defects with quenched-like disorder affecting the propagation of the DW [11,13]. Because of such a high quality of the films, magnetization reversal is characterized by easy DW motion, following rare nucleation events. Our group has shown [11] that these 2D films are particularly appropriate for creep process studies by measurement of an exponent $\mu = 1/4$ in very good agreement with the theoretical predictions.

Following previous studies [5], we used the extraordinary Hall effect to detect with a very high sensitivity the propagation of a single DW in submicron size wires. Double symmetric Hall cross devices were patterned using electron beam lithography and ion beam etching. As can be seen in the magneto-optic (MO) image in Fig. 1, a single DW was injected into the device by adjoining a large nucleation area [5,21] to one of the current probes. When entering into the wire, the single DW behaves as a

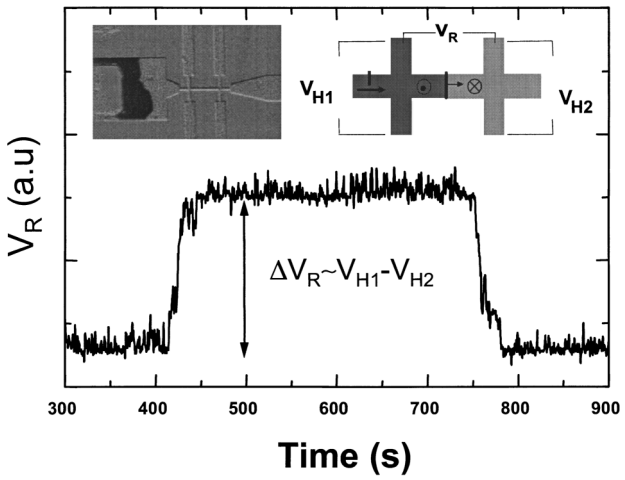

FIG. 1. Time dependence of the longitudinal voltage V_R during magnetization reversal. The first (second) step corresponds to the DW moving inside the first (second) cross. The inset shows the sketch of voltage measurement and a MO image indicating a single domain nucleation in the large magnetic area ($t_{Co} = 1$ nm).

1D nano-object propagating in a confined 2D geometry [5]. By measuring the time dependence of V_R in a fixed field H, and using the fact that V_R is proportional to the extraordinary Hall voltage difference $V_{H1} - V_{H2}$, one can precisely deduce the average DW velocity $v(H)$ inside the connecting wire as can be seen in Fig. 1. Results are shown in Fig. 2(a) where $\log v(H)$ vs $H^{-1/4}$ is plotted for four different wire widths ranging from 0.5 to 1.5 μm patterned in a 1 nm thick Co layer. Surprisingly, we observe a huge reduction of the velocity $v(H)$ when the wire width is reduced, which indicates an increase of the energy barrier for DW motion. For all widths, the straight lines of Fig. 2(a) indicate that the data are compatible with a creep formula $v(H) = v_0 \exp(-\beta U_{cw}(H_{cw}/H)^{1/4})$, where H_{cw} and U_{cw} are, respectively, the critical field and the scaling energy constant in the wire. Note that we have also tested $\log v(H)$ vs $(1 - H/H_{cw})^{\alpha}$ and $(H_{cw}/H)^{\mu}$ for α and μ values ranging from 0.05 to 1. The value $\mu = 1/4$, which was already found in similar but unpatterned continuous films [9,11], is expected in the case of a one dimensional interface moving in one transverse direction. The width $w_0 = 1.5$ μm corresponds to the highest velocity and a curvature at high fields is observed which suggests that the system leaves the creep regime. Figure 2(b) indicates that the effective critical field $H_c^{\text{eff}} = (\beta U_{cw})^4 H_{cw}$ deduced from the slope of the curves in Fig. 2(a) scales as $(1/w_0)$. This dependence leads us to believe that the reduction of $v(H)$ is induced by a mechanism linked to the edges of the magnetic wires. Since H_c^{eff} reflects the strength of the pinning potential, we have checked the quality of the wires by using scanning electron microscopy. Although no patterning-induced major defects are visible, for all wires a slight sinusoidal-like edge roughness (period ~ 200 nm; amplitude ~ 20 nm) is present which is more or less symmetric on both sides of the wire.

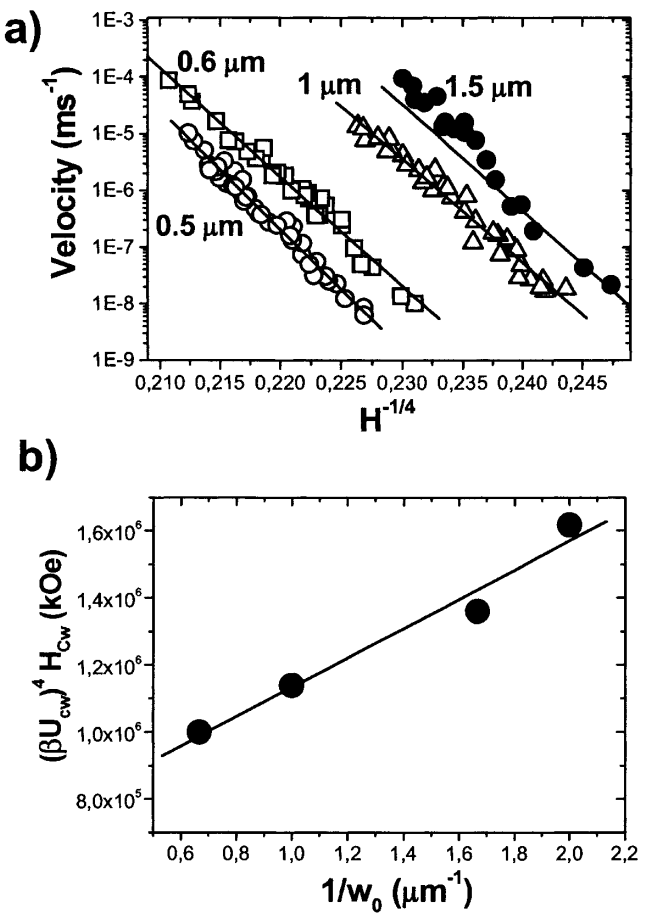

FIG. 2. (a) Average DW velocity as a function of $H^{1/4}$ for 1.5, 1, 0.6, and 0.5 μm wide wires patterned in a 1 nm thick Co layer. (b) Effective critical field H_c^{eff} as a function of $(1/w_0)$.

We now show that such an edge roughness (ER) can lead to the $1/w_0$ dependence observed in Fig. 2(b). As seen in Fig. 3(a), we have fabricated wires with strong artificially induced ER of the simple form $w(x) = w_0 + 2a|\sin(kx)|$ (x is the position along the wire, $w(x)$ is the wire width, w_0 is a constant width, a is the amplitude of the roughness, and $k = \pi/p$ is its wave vector) by contacting lithographically made circles. Figure 3(b) shows $\log v(H)$ vs $H^{-1/4}$ for a wire of width $w_0 = 1$ μm exhibiting either natural roughness ($a = 10$ nm and $p = 200$ nm) or strong artificial roughness ($a = 200$ nm and $p = 1$ μm), compared to the dependence inside the large reservoir assumed to display the intrinsic properties of the nonpatterned film (as determined by a MO microscopy study). The three velocity measurements have been done in the same sample patterned in a 0.5 nm thick Co layer. We observe a reduction of the DW velocity inside the "natural" wire by about 1 order of magnitude with respect to the reservoir. This clearly indicates that additional pinning effects drive the DW dynamics in magnetic wires. But the most important feature is that

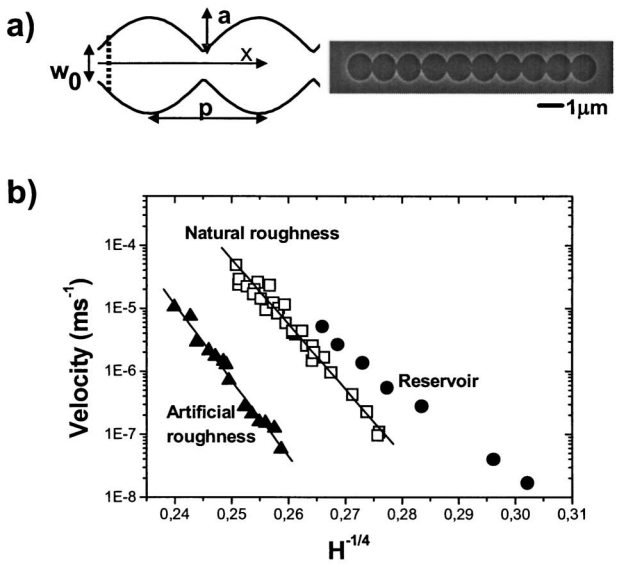

FIG. 3. (a) DW propagating in a wire where the lateral width is varying as $w(x) = w_0 + 2a|\sin(kx)|$ and scanning electron microscopy (SEM) image after the resist writing process of a wire with artificial ER of form $w(x)$ ($a = 200$ nm; $p = 1$ μm). (b) Average DW velocity inside a wire of 1 μm with natural ER ($a = 10$ nm; $p = 200$ nm) and with artificially induced ER (a) patterned in the same 0.5 nm thick Co layer, compared to the DW velocity inside the large reservoir.

the velocity is further reduced by the presence of the strong artificial ER. This result is a striking confirmation of the influence of edge modulation on DW dynamics. The data for the wires with natural and artificial roughness are also consistent with the creep formula with $\mu = 1/4$, whereas in the reservoir for the same field range a different thermally activated behavior due to a lowest energy barrier is observed.

Next we discuss how the ER can influence DW creep in the magnetic wires. The first possibility is that ER could lead to additional "intrinsic" pinning. Typically, a defect can pin the DW only if its spatial extension along the direction of propagation is of the order of the DW width $\Delta \sim 10$ nm [7]. However, as the typical extension of the edge roughness p is much larger than Δ (here $p \geq 200$ nm), the ER cannot lead to intrinsic pinning. Another possibility is a topological effect due to the roughness-induced modulation of the DW length when the DW propagates along the wire. In the following, we show that such a variation of the DW length can be taken into account by introducing a position dependent *macroscopic* field. Consider a straight DW of length L reaching the input of a magnetic wire of width $w(x)$ [Fig. 3(a)]. To propagate under an applied field H, the DW has to change its length. First, let us neglect the presence of intrinsic structural defects. Its static properties can be energetically described by the balance between wall energy (which favors a reduction of the wall length) and Zeeman energy (increasing the reversed area). If the DW center propagates by dx and the corresponding reversed surface is dS, the wall energy and Zeeman energy variations are $dE_\sigma = \sigma t_{\mathrm{Co}}(\partial L/\partial x)dx$, where $\sigma = 4(AK_{\mathrm{eff}})^{1/2}$ is the wall energy per unit surface (A is the exchange stiffness), and $dE_Z = -2M_S H t_{\mathrm{Co}}(\partial S/\partial x)dx$. The change of total energy is $dE_{\mathrm{tot}}/dx = \sigma t_{\mathrm{Co}}(dL/dx) - 2M_S H t_{\mathrm{Co}}(dS/dx)$. This energy is minimized at a given position x of the wire by the field

$$H_{\mathrm{top}}(x) = \frac{\sigma}{2M_s}\left(\frac{dL}{dS}\right)_x. \tag{1}$$

This topological field is either positive when $dw/dx > 0$ ($dL > 0$) or negative when $dw/dx < 0$ ($dL < 0$). If $dw/dx \gg 1$, the DW is bent [5,22]. Here, however, as $w(x)$ varies smoothly (the aspect ratio $a/p \ll 1$ is small), it is a good approximation to consider that the DW remains straight; i.e., $L(x) = w(x)$. Now let us consider how this topologically induced field $H_{\mathrm{top}}(x)$ can lead to the observed creep process using an approach from collective pinning theory developed for vortices in superconductors [7]. In an unpatterned film, the total free-energy functional for a segment L of a DW moving in the x direction under an external force F per unit surface is [9]

$$E(u) = \varepsilon_{\mathrm{el}}\frac{u^2}{L} - (\xi^2 L\gamma)^{1/2} - F t_{\mathrm{Co}} L\frac{u}{2}, \tag{2}$$

where $u(x)$ denotes the amplitude of the displacement of this segment, $\varepsilon_{\mathrm{el}} = \sigma t_{\mathrm{Co}}$ is the elastic tension per unit length, γ scales the pinning strength of the disorder, and ξ is the characteristic length of the disorder. The first and second terms are the elastic and the pinning energies, respectively. This equation is used to describe the energy involved in DW propagation as a succession of rigid microscopic segments of length L_c (Larkin length) interacting with a quenched disorder over a typical length scale ξ. This equation neglects the DW bending and is valid only for $F \sim F_c$, where F_c is the critical force. In an unpatterned magnetic film, the last term is simply the Zeeman energy given by $-M_s tLuH$. The way to take into account the influence of the edge modulation in Eq. (2) is to consider a DW of length L which propagates under the action of a macroscopic external field $H - H_{\mathrm{top}}(x)$, where $H_{\mathrm{top}}(x)$ is given by Eq. (1) (the sign is negative since a positive topological field acts as a restoring force). The total force term in Eq. (2) is thus $-M_s tLu(H - H_{\mathrm{top}}(x))$. By minimizing $E(u)$ for $H = 0$ and setting $u = \xi$ [9] for each position x one gets the position dependent collective pinning length in the wire $L_{cw}(x)$, beyond which the DW adjusts elastically to the potential in order to reach an optimal local configuration. To first order we find $L_{cw}(x) \approx L_c\{1 + \frac{2}{3}[H_{\mathrm{top}}(x)/H_c]\}$, where $L_c = (\varepsilon_{\mathrm{el}}^2\xi^2/\gamma)^{1/3}$ and $H_c = (\varepsilon_{\mathrm{el}}\xi/M_S t)(1/L_c)^2$ are, respectively, the Larkin length and the critical field due to the quenched disorder in the nonpatterned film (in our films ξ and L_c can be estimated to be 30 nm and 50 nm, respectively). This shows that the straightness of the DW can be artificially tuned by tailoring $H_{\mathrm{top}}(x)$. Finally, the critical

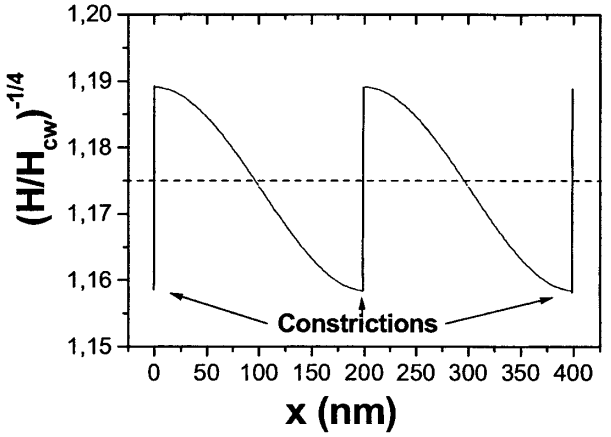

FIG. 4. Typical potential landscape $(H_{cw}/H)^{1/4}$ vs x (for $H =$ 200 Oe and $H_c \sim 400$ Oe) for the wire of natural roughness of Fig. 3(b). The dashed line represents the potential without ER.

field H_{cw} of the wire is found by equating the force and the pinning terms for $L = L_{cw}$ [7]. This immediately leads to $H_{cw}(x) = H_c + H_{\text{top}}(x)$. Thus the creep law can be renormalized by introducing an effective critical field $H_{cw}(x)$ which is simply the sum of the critical field due to the quenched disorder and a topologically induced field due to the modulation of the DW length; i.e., $v(H) = v_0 \exp\{-\beta U_{cw}[(H_c + H_{\text{top}}(x))/H]^{1/4}\}$.

As an example, Fig. 4 shows a typical creep potential landscape $[H_{cw}(x)/H]^{1/4}$ vs x calculated by using Eq. (1) for a straight DW of length $L(x) = w_0 + 2a|\sin(kx)|$. The potential presents a valley at each constriction. At this position, the DW has to overcome an energy barrier which is maximum because $H_{\text{top}}(x)$ reaches its highest value $H_{\text{top}}^{\max}$. Equation (1) with this $L(x)$ yields $H_{\text{top}}^{\max} = (\sigma/M_s)(ka/w_0)$ ($H_{\text{top}}^{\max} \sim 20$ Oe for the natural ER and $\sim$70 Oe for the artificial one). This indicates that the constrictions can be considered as the most favorable metastable states inside the magnetic wire as we have checked by quasistatic MO measurements. In the creep regime, when $H \ll H_{cw}$ larger DW segments [scaling as $L_{\text{opt}} \approx L_{cw}(H_{cw}/H)^{3/4}$] and longer DW hops [scaling as $u(L_{\text{opt}}) = u_c(L_{\text{opt}}/L_{cw})^{2/3}$] are involved in order to find the next favorable metastable state [7]. As $H_{\text{top}}(x) \ll H_c$ (here $H_c \sim$ 300–900 Oe), then $L_{cw}(x) \approx L_c$. Considering an applied field $H \sim H_c/4$, $u_c \sim \xi \sim 30$ nm and $L_c \sim$ 50 nm, we estimate $L_{\text{opt}} \sim 140$ nm and $u(L_{\text{opt}}) \sim 60$ nm. In the wires, the DW is thus made of a few segments and jumps only a few times between each constriction. One can consider that at position x a hop between two metastable states takes an average time given by $\tau(H, x) \propto \exp[\beta U_{cw}(H_{cw}(x)/H)^{1/4}]$, so that the total average time measured in our experiment (Fig. 1) is mainly dominated by the longer times needed to overcome the energy barrier at constrictions where H_{cw} is maximum. A good approximation is thus to consider that the critical field in the wire is simply $H_c + H_{\text{top}}^{\max} = H_c + (\sigma/M_s)(ka/w_0)$. The most striking result is that H_{cw} is found to be proportional to $1/w_0$ which is in agreement with the experimental results of Fig. 2(b). Finally, we estimate the experimental (theoretical) ratio $S_{\text{exp(theo)}} = H_{cw}(\text{natural})/H_{cw}(\text{artificial})$ for the wires with natural and artificial roughness of Fig. 3(b). We find values $S_{\text{exp}} = 0.88 \pm 0.05$ and $S_{\text{theo}} = 0.94$ which are in reasonable correspondence.

In summary, we have shown that in magnetic wires, due to the ER, the creep process is renormalized with respect to a nonpatterned film by introducing an effective critical field proportional to $1/w_0$. As a consequence the edge modulation can be artificially tuned to control precisely the DW motion and the DW straightness. These features are promising for applications to high density magnetic logic devices and high density magnetic recording.

R. Stamps is gratefully acknowledged for crucial suggestions. We acknowledge financial support by NEDO contract "Nanopatterned magnet."

*Corresponding author.
Electronic address: dafine.ravelosona@ief.u-psud.fr

[1] D. A. Allwood *et al.*, Science **296**, 2003 (2002).
[2] R. Richter *et al.*, Appl. Phys. Lett. **80**, 1291 (2002).
[3] W. C. Black, Jr. and B. Das, Jr., J. Appl. Phys. **87**, 6674 (2000).
[4] T. Ono *et al.*, Science **284**, 468 (1999).
[5] J. Wunderlich *et al.*, IEEE Trans. Magn. **37**, 2104 (2001).
[6] J. P. Jamet *et al.*, IEEE Trans. Magn. **37**, 2120 (2001).
[7] G. Blatter *et al.*, Rev. Mod. Phys. **66**, 1125 (1994).
[8] T. Tybell, P. Paruch, T. Giamarchi, and J. M. Triscone, Phys. Rev. Lett. **89**, 097601 (2002).
[9] S. Lemerle *et al.*, Phys. Rev. Lett. **80**, 849 (1998).
[10] X. Krusin-Elbaum *et al.*, Nature (London) **410**, 444 (2001).
[11] T. Shibauchi *et al.*, Phys. Rev. Lett. **87**, 267201 (2001).
[12] M. Kardar, Physica (Amsterdam) **221B**, 60 (1996).
[13] G. Gruner, Rev. Mod. Phys. **60**, 1129 (1988).
[14] D. Wilkinsion and J. F. Willemsen, J. Phys. A **16**, 3365 (1983).
[15] M. V. Feigel'man, V. B. Geshkenbein, A. I. Larkin, and V. M. Vinokur, Phys. Rev. Lett. **63**, 2303 (1989).
[16] E. T. Seppala and M. J. Alava, Phys. Rev. Lett. **84**, 3982 (2000).
[17] E. T. Seppala, M. J. Alava, and P. M. Duxbury, Phys. Rev. E **63**, 36126 (2001).
[18] V. Mathet *et al.*, J. Magn. Magn. Mater., **260**, 295 (2003).
[19] Y. Yafet and E. M. Gyorgi, Phys. Rev. B **38**, 9145 (1988).
[20] J. Ferre, *Spin Dynamics in Confined Magnetic Structures I* (Springer-Verlag, Berlin, Heidelberg, 2002), Vol. 83, p. 127.
[21] F. Fournel *et al.*, IEEE Trans. Magn. **34**, 1027 (1998).
[22] D. Ravelosona *et al.*, J. Magn. Magn. Mater. **249**, 170 (2002).